Phytochemistry Letters 35 (2020) 206–210

Contents lists available at ScienceDirect

Phytochemistry Letters

journal homepage: www.elsevier.com/locate/phytol

Induced production of zinniol analogues by co-cultivation of two endophytic fungi in the same ecological niche

Zi-Ru Wang[a], Hong-Xia Yang[a], Xiao-Ping Peng[a], Gang Li[a,*], Hong-Xiang Lou[a,b,*]

[a] Department of Natural Medicinal Chemistry and Pharmacognosy, School of Pharmacy, Qingdao University, Qingdao, 266021, People's Republic of China
[b] Department of Natural Product Chemistry, Key Laboratory of Chemical Biology of Ministry of Education, School of Pharmaceutical Sciences, Shandong University, Jinan, 250012, People's Republic of China

ARTICLE INFO

Keywords:
Endophytes
Co-cultivation
Secondary metabolites
Zinniol analogues
Bioactivity

ABSTRACT

Three zinniol analogues, pleoniols A–C (**1**–**3**), together with a known compound (**4**), were isolated from a mixed fermentation of two endophytic fungi, *Pleosporales* sp. F46 and *Acremonium pilosum* F47, both of which are found the pedicel of the medicinal plant *Mahonia fortunei*. High-performance liquid chromatography analysis showed that none of compounds **1**–**4** were detected when either one of the two fungi was cultured alone. The structures of compounds **1**–**4**, including the absolute configurations, were deduced based on the interpretation of HRMS, NMR, and optical rotation data. Compounds **1**–**3** exhibited no antimicrobial efficacies against four Gram-positive or Gram-negative bacteria and two plant pathogenic fungi. Moreover, they demonstrated no obvious cytotoxic activities against four cancer cell lines, A549, MDA-MB-231, CT-26 and MCF-7. Our work indicates that the co-culture of endophytes in the same ecological niche is an effective approach for promoting interspecies interaction and enriching chemical diversity.

1. Introduction

Endophytic fungi have been proven to be an important source of natural products with unique structures and significant biological activities (Aly et al., 2013; Gao et al., 2018). However, under the standard laboratory culture conditions, most of their biosynthetic gene clusters (BGCs) are silent, and many cryptic secondary metabolites have not been explored (Rutledge and Challis, 2015; Scherlach and Hertweck, 2009). To date, some strategies have been developed to activate silent BGCs to obtain novel natural products (Li and Lou, 2018). Among them, co-cultivation is well-known as an effective approach to induce the expression of BGCs through promoting interspecies interaction (Marmann et al., 2014; Chen et al., 2015). A plethora of traits, such as bioactive product formation (Wang et al., 2019), are typically involved in the interspecies interaction and improve the richness of microbial metabolites.

Recently, an endophytic fungus *Pleosporales* sp. F46, was isolated from the pedicel of the medicinal plant *Mahonia fortunei* by our research group (Li et al., 2019). Its rice culture fermentation afforded seven new heptaketides with antifungal or cytotoxic activities (Li et al., 2019). To maximize the chemical diversity of this fungal endophyte by promoting interspecies interaction, the co-cultivation of *Pleosporales* sp. F46 with the endophytic bacterium *Bacillus wiedmannii* Com1 was carried out, and a new antibacterial ergosterol was discovered (Wang et al., 2019). By further considering the interspecies interaction between endophytes in the same ecological niche, the endophytic fungus *Acremonium pilosum* F47, also isolated from the pedicel of *M. fortunei*, was selected for co-cultivation with *Pleosporales* sp. F46 in our current work. Herein, we report the isolation, characterization, and antibacterial evaluation of three new zinniol analogues, pleoniols A–C (**1**–**3**), via the co-cultivation of *Pleosporales* sp. F46 with *A. pilosum* F47.

2. Results and discussion

In the pre-screening period, the EtOAc extracts from the co-culture and axenic fermentations of endophytes in PDB media were analysed. HPLC-based metabolic profiling was performed to compare their metabolomes (Fig. 1). Several compounds were only detected when the endophytic fungus *Pleosporales* sp F46 was co-cultivated with *A. pilosum* F47 (Fig. 1), implying that several BGCs were activated. Further feeding experiments performed by adding sterilized fungal materials to culture media suggested that the formation of the abovementioned compounds was very likely due to the fungal interspecies interaction (Fig. 1). To obtain these potential bioactive compounds formed in the interspecies

* Corresponding authors at: Department of Natural Medicinal Chemistry and Pharmacognosy, School of Pharmacy, Qingdao University, Qingdao, 266021, People's Republic of China.
E-mail addresses: gang.li@qdu.edu.cn (G. Li), louhongxiang@sdu.edu.cn (H.-X. Lou).

https://doi.org/10.1016/j.phytol.2019.12.007
Received 16 October 2019; Received in revised form 22 November 2019; Accepted 16 December 2019

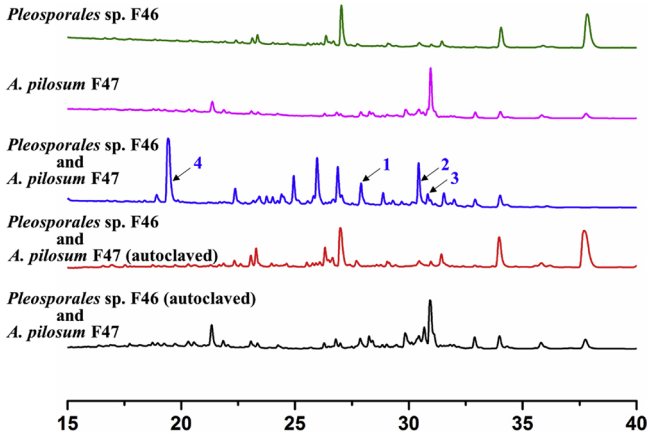

Fig. 1. HPLC-DAD profiles (210 nm) of ethyl acetate extracts of the culture of *Pleosporales* sp. F46, the culture of *A. pilosum* F47, the co-culture of *Pleosporales* sp. F46 and *A. pilosum* F47, the culture of *Pleosporales* sp. F46 by feeding sterilized fungal material from *A. pilosum* F47, and the culture of *A. pilosum* F47 by feeding sterilized fungal material from *Pleosporales* sp. F46.

interaction process, the EtOAc extract of the co-culture was fractionated by flash chromatography, gel permeation chromatography (GPC) on Sephadex LH-20, and semi-preparative HPLC to afford compounds **1**–**4**, which were not detected when the endophyte was cultured alone or cultured with autoclaved fungal materials (Fig. 1).

Compound **1** (Fig. 2) was isolated as a colourless powder, and possessed a molecular formula of $C_{21}H_{32}O_8$ as determined by ESI-HRMS. The ^{1}H NMR spectrum of **1** (Fig. S1) showed the presence of five singlet methyl groups (δ_H 1.66, 1.75, 2.11, 2.22, and 2.22), one olefinic proton (δ_H 5.52), and the remaining oxygenated methylenes or methines. Its ^{13}C NMR spectrum (Fig. S2) exhibited 21 carbon signals including two oxygenated aromatic/olefinic carbons (δ_C 151.5, and 155.2). The 1D NMR data (Table 1) in combination with the HSQC spectrum (Fig. S4) established five singlet methyl groups, three oxygenated methylenes, and five oxygenated methines, together with eight olefinic/aromatic carbons including one methine.

Interpretation of the ^{1}H-^{1}H COSY NMR spectrum (Fig. S3) identified connections between C-1′ and C-2′, and C-1″ to C-6″, indicating the presence of a sugar motif in the structure. The structure of compound **1** was further constructed according to the HMBC NMR data (Fig. S5). Key HMBC correlations of H_2-10 with C-1, C-5, and C-6, H_3-7 with C-1, C-2, and C-6, H_3-8 with C-1, C-2, and C-3, and H_3-9 with C-3, C-4, and C-5 identified a benzene ring substituted with three methyls at C-1, C-2, and C-4 (Fig. 3). In addition, an oxygenated methylene (C-10) was attached to C-6 of the aromatic ring. An oxygenated dimethylallyl group

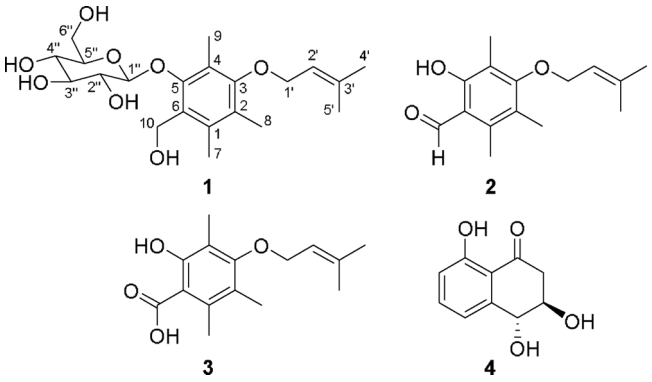

Fig. 2. Chemical structures of compounds **1**–**4**.

was revealed and was connected to C-3, which was supported by the HMBC correlations of H_3-4′/C-2′, H_3-4′/C-3′, H_3-4′/C-5′, H_3-5′/C-2′, H_3-5′/C-3′, and H_3-5′/C-4′, as well as the key HMBC correlation of H_2-1′/C-3 (Fig. 3). The strong HMBC correlation between H-1″ and C-5 was used to place the sugar moiety at C-5 through an oxygen bridge (Fig. 3). Thus, the planar structure of compound **1** (Fig. 2) was verified as a zinniol analogue (Zhu et al., 2017), which was also in accordance with the MS data.

The absolute configuration of the sugar motif was determined by the measurement of the optical rotation (He et al., 2019; Wu et al., 2019). Acid hydrolysis of **1** provided D-glucose, which was identified by direct comparison with an authentic sample (Experimental Section and Fig. S25). Therefore, the structure of compound **1** was established accordingly. Compound **1** was assigned the name pleoniol A.

Compound **2** (Fig. 2) was also isolated as a colourless powder. It had a molecular formula of $C_{15}H_{20}O_3$ according to ESI-HRMS. The ^{1}H NMR spectrum of **2** (Fig. S10) indicated the presence of five singlet methyl groups (δ_H 1.71, 1.81, 2.16, 2.17, and 2.47), one oxygenated methylene (δ_H 4.29, d, J =7.0 Hz), one olefinic/aromatic proton (δ_H 5.58, t, J =7.0 Hz), and two remaining singlet protons at δ_H 10.3 and 12.5. The ^{1}H NMR data with the aid of ^{13}C NMR and HSQC spectra of **2** (Figs. S11 and S12) identified five singlet methyl groups, one methylene group (oxygenated), and an aldehyde group (δ_H 10.3; δ_C 194.7), together with eight aromatic/olefinic carbons including one methine (δ_C 119.8), and two oxygenated quaternary carbons (δ_C 161.7, and 163.4). The above data for compound **2** suggested highly similar structural features to those of compound **1**, except for the absence of one oxygenated methylene and a sugar moiety. Considering the key HMBC correlations between H-10 and C-5 and C-6 and between H_3-7 and C-6, as well as the chemical shift of C-10, the aldehyde group in **2** instead of the oxygenated methylene in **1** was placed at C-6 (Fig. 3). A free hydroxyl group was placed at C-5 through the analysis of the key HMBC correlations between 5-OH and C-4, C-5, and C-6 (Fig. 3). Accordingly, the structure of compound **2** was determined. Compound **2** was named pleoniol B.

Compound **3** was obtained as a colourless powder and named pleoniol C. It was assigned the molecular formula $C_{15}H_{20}O_4$, showing it had one additional oxygen atom compared with **2**. Moreover, the ^{1}H and ^{13}C NMR spectra of compound **3** (Figs. S17 and S18) showed that its structure was similar to that of **2**, except for the absence of H-10 and 5-OH in the ^{1}H NMR spectrum of **3**, and the upfield shift of C-10 in the ^{13}C NMR spectrum of **3**. The analysis of the above difference indicated that the carboxyl group in **3**, instead of the aldehyde moiety in **2**, was located at C-6, which was also supported by the 2D NMR data (Fig. 3 and Figs. S19–S21). The structure of the known compound **4** was elucidated as (3*R*,4*R*)-3,4-dihydro-3,4,8-trihydroxy-1(2*H*)-naphthalenone based on comparison of its NMR and CD data (Fig. S27) with those reported in the literature (Borgschulte et al., 1992; Wu et al., 2019).

Zinniol and its analogues are tetraketide-derived compounds and are frequently found in *Alternaria* species (Gamboa-Angulo et al., 2002; Lou et al., 2013). In addition to their well-known phytotoxic effects (Stierle et al., 1993), they have also been reported to have antifungal activity (Yang et al., 2011), and anti-virus efficacy (Ai et al., 2012). New compounds **1**–**3**, as zinniol analogues (Zhu et al., 2017; Bitchi et al., 2019), were screened for their antibacterial activities against the Gram-positive bacteria *Staphylococcus aureus* (ATCC 6538) and *Bacillus subtilis* (ATCC 9372) along with the Gram-negative bacteria *Pseudomonas aeruginosa* (ATCC 27853) and *Escherichia coli* (ATCC 25922), and their antifungal activities against two plant pathogens, *Colletotrichum musae* [ACCC (Agricultural Culture Collection of China) 31244] and *Colletotrichum coccodes* (ACCC 36067), were determined. Furthermore, their cytotoxic activities against the A549, MDA-MB-231, CT-26, and MCF-7 cancer cell lines were also evaluated. Unfortunately, in contrast to the positive controls, none of the compounds were effective at the given concentrations against the tested microorganisms or cancer cells.

Table 1
^{1}H and ^{13}C NMR Data for Compounds **1–3**.

Position	**1**			**2**			**3**		
	δ_C, mult.[a]	δ_H mult.[b] (*J* in Hz)	Key HMBC	δ_C, mult.[c]	δ_H mult.[d] (*J* in Hz)	Key HMBC	δ_C, mult.[c]	δ_H mult.[d] (*J* in Hz)	Key HMBC
1	135.2, C_q			138.7, Cq			138.5, Cq		
2	126.0, C_q			121.9, Cq			122.1, Cq		
3	155.2, C_q			163.4, Cq			160.8, Cq		
4	121.2, C_q			117.1, Cq			116.6, Cq		
5	151.5, C_q			161.7, Cq			160.5, Cq		
6	129.6, C_q			115.4, Cq			108.6, Cq		
7	15.5, CH_3	2.22, s	1, 2, 6	13.9, CH_3	2.47, s	1, 2, 6	18.8, CH_3	2.49, s	1, 2, 6
8	12.6, CH_3	2.11, s	1, 2, 3	12.2, CH_3	2.17, s	1, 2, 3	12.9, CH_3	2.18, s[e]	1, 2, 3
9	10.3, CH_3	2.22, s	3, 4, 5	8.7, CH_3	2.16, s	3, 4, 5	9.4, CH_3	2.18, s[e]	3, 4, 5
10	55.6, CH_2	4.36, d (11.0) 4.73, d (11.0)	1, 5, 6	194.7, CH	10.3, s	5, 6	174.7, Cq		
1′	68.7, CH_2	4.15, dd (11.0, 7.0) 4.21, dd (11.0, 7.0)	3, 2′	69.6, CH_2	4.29, d (7.0)	3, 2′	69.5, CH_2	4.25, d (7.0)	3, 2′
2′	120.6, CH	5.52, t (7.0)	1′, 3′, 4′, 5′	119.8, CH	5.58, t (7.0)	1′, 3′, 4′, 5′	120.0, CH	5.58, t (7.0)	1′, 3′, 4′, 5′
3′	136.6, C_q			138.6, Cq			138.3, C_q		
4′	25.5, CH_3	1.75, s	2′, 3′, 5′	25.9, CH_3	1.81, s	2′, 3′, 5′	25.9, CH_3	1.80, s	2′, 3′, 5′
5′	17.8, CH_3	1.66, s	2′, 3′, 4′	18.0, CH_3	1.71, s	2′, 3′, 4′	18.0, CH_3	1.71, s	2′, 3′, 4′
1″	104.1, CH	4.42, d (8.0)	5, 2″, 5″						
2″	74.0, CH	3.29, t (8.0)	1″, 3″						
3″	76.3, CH	3.23, t (8.0)	2″, 4″						
4″	70.6, CH	3.05, m[e]	3″, 5″						
5″	76.4, CH	3.04, m[e]	4″, 6″						
6″	61.5, CH_2	3.67, d (10.5) 3.36, m[e]	5″						
5-OH					12.5, s	4, 5			

[a] Recorded in DMSO-d_6 at 125 MHz.
[b] Recorded in DMSO-d_6 at 500 MHz.
[c] Recorded in $CDCl_3$ at 125 MHz.
[d] Recorded in $CDCl_3$ at 500 MHz.
[e] Overlapped.

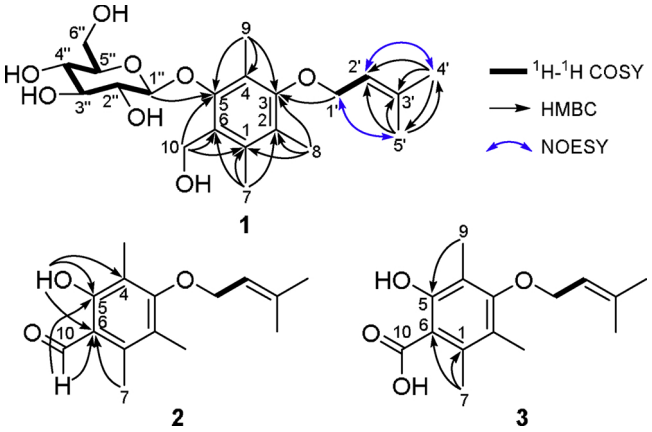

Fig. 3. Key ^{1}H-^{1}H COSY and HMBC correlations of compounds **1–3**.

3. Experimental section

3.1. General experimental procedures

NMR spectra were recorded on a Bruker Advance spectrometer operating at 500 (^{1}H) and 125 (^{13}C) MHz. Mass spectra were obtained with an LTQ-Orbitrap spectrometer equipped with an ESI source. Optical rotation was measured on a Jasco P-1020 digital polarimeter (JASCO Corporation, Tokyo, Japan). IR spectra were obtained using a Cary 600 Series FTIR spectrometer (Agilent Technologies, Germany). Flash chromatography was performed on a Teledyne ISCO CombiFlash Rf 200 system equipped with a C18 spherical column (20 − 35 μm, 100 Å, 80 g). The semi-preparative HPLC system (Agilent 1260 Infinity II, Agilent Technologies, Germany) was equipped with a ZORBAX SB-C18 column (4.6 × 250 mm) or an Eclipse XDP-C18 column (9.4 × 250 mm). Silica gel (200–300 mesh; Qingdao Haiyang Chemical Co., Ltd., China) and Sephadex LH-20 (25 − 100 μm; Pharmacia, Uppsala, Sweden) were used for column chromatography (CC). Thin-layer chromatography (TLC) was performed with silica gel GF_{254} plates (Qingdao Haiyang Chemical Co., Ltd., China).

3.2. Fungal material

The fungal endophytes *Pleosporales* sp. F46 and *A. pilosum* F47 were both isolated from the pedicel of the medicinal plant *M. fortunei*, which was collected from Qingdao, People's Republic of China. The identification of the endophytic fungus *Pleosporales* sp F46 has been described previously (Li et al., 2019). The endophytic fungus *A. pilosum* F47 was characterized by internal transcribed spacer (ITS) sequencing and its ITS sequence has been deposited at GenBank (accession number MN294707). The above fungi were deposited at the School of Pharmacy, Qingdao University, People's Republic of China. For large-scale fermentation, the fungus *Pleosporales* sp. F46 or *A. pilosum* F47 was first cultured in 30 Erlenmeyer flasks (500 mL) each containing 100 mL of potato dextrose broth (PDB), on a rotary shaker (150 rpm) at 28 °C for 5 d. Then, the above PDB cultures from *Pleosporales* sp. F46 and *A. pilosum* F47 were mixed, and further incubated at 28 °C for 15 d in a shaker (150 rpm). For more details, please see Fig. S26 in the Supporting Information.

3.3. Extraction and isolation

The entire fermentation was filtered through cheese cloth to separate the supernatant from the mycelia. The supernatant was extracted with ethyl acetate (EtOAc) by sonication at room temperature and then evaporated under reduced pressure to yield a crude gum (3.8 g). The extract was separated by flash chromatography and eluted with MeOH–H_2O (5 % MeOH for 5 min, followed by a gradient of 5–100 %

MeOH over 55 min and 100 % MeOH for 25 min). All fractions were combined to provide four major fractions (A–D) based on TLC analyses. Based on the HPLC analyses, fractions containing secondary metabolites that were detected only in the co-cultivation condition were subjected to isolation and purification. Fraction A (65.0 mg) was directly purified by semi-preparative HPLC (ZORBAX SB-C18 column, MeOH-H_2O-0.1 % FA, 70/30, 1.0 mL/min) to yield compound **4** (11.2 mg, t_R = 10.5 min). Fraction B (116.0 mg) was applied to the Sephadex LH-20 GPC (MeOH) to yield four subfractions (B1-B4). Subfraction B3 (36.0 mg) was further purified by semi-preparative HPLC (ZORBAX SB-C18 column, MeOH-H_2O-0.1 % FA, 57/43, 1.0 mL/min) to provide compound **1** (10.1 mg, t_R = 12.5 min). Fraction C (101.3 mg) was also applied to the Sephadex LH-20 GPC (MeOH) to yield four subfractions (C1-C4). Subfraction C3 (13.2 mg) was purified by semi-preparative HPLC (Eclipse XDP-C18 column, MeOH-H_2O-0.1 % FA, 77/23, 2.0 mL/min) to generate compound **3** (2.7 mg, t_R = 31.0 min). By following a similar isolation procedure as that used for fractions B and C, fraction D (51.3 mg) was fractionated by a Sephadex LH-20 column (MeOH) and purified by semi-preparative HPLC (Eclipse XDP-C18 column, MeOH-H_2O-0.1 % FA, 86/14, 2.0 mL/min) to afford compound **2** (1.9 mg, t_R = 20.0 min).

3.3.1. Pleoniol A (1)

Colourless powder; [α]20 D = -11.9 (*c* 0.10, MeOH); UV λ_{max} 202 nm; IR ν_{max} 3515, 3410, 3278, 2914, 1687, 1370 cm^{-1}; ^1H NMR (500 MHz, DMSO-d_6) and ^{13}C NMR (125 MHz, DMSO-d_6), see Table 1; (+)-ESI-HRMS *m/z*: 435.1981 $[M+Na]^+$ (calcd. for $C_{21}H_{32}O_8Na$, 435.1989, Δ −1.8818 ppm), *m/z*: 395.2059 $[M+H-H_2O]^+$ (calcd. for $C_{21}H_{31}O_7$, 395.2064, Δ −1.3351 ppm), *m/z*: 847.4087, $[2M+Na]^+$ (calcd. for $C_{42}H_{64}O_{16}Na$, 847.4087, Δ 0.0408 ppm).

3.3.2. Pleoniol B (2)

Colourless powder; UV λ_{max} 216, 286, 354 nm; IR ν_{max} 3733, 2917, 1626, 1421, 1314 cm^{-1}; ^1H NMR (500 MHz, $CDCl_3$) and ^{13}C NMR (125 MHz, $CDCl_3$), see Table 1; (-)-ESI-HRMS *m/z*: 247.1338 $[M-H]^-$ (calcd. for $C_{15}H_{19}O_3$ 247.1340, Δ -0.5729 ppm).

3.3.3. Pleoniol C (3)

Colourless powder; UV λ_{max} 216, 258, 316 nm; IR ν_{max} 3443, 2927, 1633, 1596, 1378 cm^{-1}; ^1H NMR (500 MHz, $CDCl_3$) and ^{13}C NMR (125 MHz, $CDCl_3$), see Table 1; (+)-ESI-HRMS *m/z*: 265.1436 $[M+H]^+$ (calcd. for $C_{15}H_{21}O_4$ 265.1434, Δ 0.6792 ppm).

3.4. Acid hydrolysis of compound 1 and sugar analysis

Compound **1** (2.0 mg) was hydrolysed using 5 % HCl (5 mL) at 60 °C for 6 h. After completion of the reaction, the reaction was concentrated under reduced pressure. The reaction mixture was then purified by HPLC (ZORBAX SB-C18 column, MeOH-H_2O-0.1 % FA, 20/80, 1.0 mL/min) to afford the pure sugar. The pure sugar was further characterized by ESI-MS and TLC analyses (Fig. S25). Final identification of D-glucose was performed by comparison of its optical rotation with that of an authentic sample under the same conditions. Hydrolysed sugar of **1**: [α] 25 D = +50.2 (*c* 0.10, H_2O); authentic D-glucose: [α]25 D = +49.8 (*c* 0.10, H_2O).

3.5. Biological assays

The antimicrobial and cytotoxic activities of all isolated compounds were investigated by following our previously reported methods (Wang et al., 2019; Li et al., 2019). The antibacterial activities of compounds **1–3** were evaluated against the Gram-positive bacteria *Staphylococcus aureus* (ATCC 6538) and *Bacillus subtilis* (ATCC 9372) and the Gram-negative bacteria *Pseudomonas aeruginosa* (ATCC 27853) and *Escherichia coli* (ATCC 25922) using the disk diffusion assay (Wang et al., 2019). All compounds were also tested for their antifungal activities against two plant pathogens, *Colletotrichum musae* (ACCC 31244) and *Colletotrichum coccodes* (ACCC 36067). The cytotoxicities of the isolated metabolites were determined against four cancer cell lines, A549, MDA-MB-231, CT-26 and MCF-7 with the MTT method (Li et al., 2019). Streptomycin, actidione, and adriamycin were used as the positive controls for the analysis of the antibacterial, antifungal, and cytotoxic activities, respectively.

4. Conclusions

Herein, we report the isolation and characterization of three new zinniol analogues, pleoniols A–C (**1–3**), and a known polyketide (**4**), from the co-cultivation of the endophytic fungi *Pleosporales* sp. F46 with *A. pilosum* F47. None of compounds **1–4** were detected when either one of the two fungi was cultured alone. The novel compounds **1–3** were evaluated for their antimicrobial and cytotoxic activities. Unfortunately, none of them were effective at the given concentrations against the tested microorganisms or cancer cells. Our work revealed that the co-culture of endophytes from the same ecological niche promotes interspecies interaction and is an effective approach for enriching chemical diversity.

Declaration of Competing Interest

There are no competing conflicts to declare.

Acknowledgements

This work was supported by the National Natural Science Foundation of China [grant numbers 81903494 and 41706077]; and the Scientific Research Foundation of Qingdao University.

Appendix A. Supplementary data

Supplementary material related to this article can be found, in the online version, at doi:https://doi.org/10.1016/j.phytol.2019.12.007.

References

Ai, H.-L., Zhang, L.-M., Chen, Y.-P., Zi, S.-H., Xiang, H., Zhao, D.-K., Shen, Y., 2012. Two new compounds from an endophytic fungus *Alternaria solani*. J. Asian Nat. Prod. Res. 14, 1144–1148.

Aly, A.H., Debbab, A., Proksch, P., 2013. Fungal endophytes-secret producers of bioactive plant metabolites. Pharmazie 68, 499–505.

Borgschulte, K., Rebuffat, S., Trowitzsch-Kienast, W., Schomburg, D., Pinon, J., Bodo, B., 1992. Isolation and structure elucidation of hymatoxins B-E and other phytotoxins from *Hypoxylon mammatum* fungal pathogen of leuce poplars. Tetrahedron 47, 8351–8360.

Chen, H., Daletos, G., Abdel-Aziz, M.S., Thomy, D., Dai, H., Brötz-Oesterhelt, H., Lin, W., Proksch, P., 2015. Inducing secondary metabolite production by the soil-dwelling fungus *Aspergillus terreus* through bacterial co-culture. Phytochemistry Lett. 12, 35–41.

Gamboa-Angulo, M.M., Escalante-Erosa, F., Carcía-Sosa, K., Alejos-González, F., Delgado-Lamas, G., Peña-Rodríguez, L.M., 2002. Natural zinniol derivatives from *Alternaria tagetica*. isolation, synthesis, and structure-activity correlation. J. Agric. Food Chem. 50, 1053–1058.

Gao, H., Li, G., Lou, H.X., 2018. Structural diversity and biological activities of novel secondary metabolites from endophytes. Molecules 23, 646.

He, X., Wang, Y.J., Luo, R.H., Yang, L.M., Wang, L., Guo, D.L., Yang, J., Deng, Y., Zheng, Y.T., Huang, S.X., 2019. Dimeric pyranonaphthoquinone glycosides with anti-HIV and cytotoxic activities from a soil-derived *Streptomyces*. J. Nat. Prod. 82, 1813–1819.

Li, G., Lou, H.X., 2018. Strategies to diversify natural products for drug discovery. Med. Res. Rev. 38, 1255–1294.

Li, G., Xu, K., Chen, W.-Q., Guo, Z.-H., Liu, Y.-T., Qiao, Y.-N., Sun, Y., Sun, G., Peng, X.-P., Lou, H.-X., 2019. Heptaketides from the endophytic fungus *Pleosporales* sp. F46 and their antifungal and cytotoxic activities. RSC Adv. 9, 12913–12920.

Lou, J., Fu, L., Peng, Y., Zhou, L., 2013. Metabolites from *Alternaria* fungi and their bioactivities. Molecules 18, 5891–5935.

Marmann, A., Aly, A.H., Lin, W., Wang, B., Proksch, P., 2014. Co-cultivation-a powerful emerging tool for enhancing the chemical diversity of microorganisms. Mar. Drugs 12, 1043–1065.

Rutledge, P.J., Challis, G.L., 2015. Discovery of microbial natural products by activation of silent biosynthetic gene clusters. Nat. Rev. Microbiol. 13, 509–523.

Scherlach, K., Hertweck, C., 2009. Triggering cryptic natural product biosynthesis in

microorganisms. Org. Biomol. Chem. 7, 1753–1760.
Stierle, A., Hershenhorn, J., Strobel, G., 1993. Zinniol-related phytotoxins from *Alternaria cichorii*. Phytochemistry 32, 1145–1149.
Wang, Z.R., Li, G., Ji, L.X., Wang, H.H., Gao, H., Peng, X.P., Lou, H.X., 2019. Induced production of steroids by co-cultivation of two endophytes from *Mahonia fortunei*. Steroids 145, 1–4.
Wu, J.T., Zheng, C.J., Zhang, B., Zhou, X.M., Zhou, Q., Chen, G.Y., Zeng, Z.E., Xie, J.L., Han, C.R., Lyu, J.X., 2019. Two new secondary metabolites from a mangrove-derived fungus *Cladosporium* sp. JJM22. Nat. Prod. Res. 33, 34–40.
Yang, X.-L., Zhang, S., Hu, Q.-B., Luo, D.-Q., Zhang, Y., 2011. Phthalide derivatives with antifungal activities against the plant pathogens isolated from the liquid culture of *Pestalotiopsis photiniae*. J. Antibiot. 64, 723–727.
Zhu, X., Chen, J., Zhu, S., He, Y., Ding, W., Li, C., 2017. Two new compounds from *Nigrospora sphaerica* ZMT05, a fungus derivated from *Oxya chinensis* Thunber. Nat. Prod. Res. 32, 2375–2381.